THE PENNSYLVANIA STATE UNIVERSITY
SCHREYER HONORS COLLEGE

DEPARTMENT OF CHEMICAL ENGINEERING

First Principles Kinetic Modeling and Reactor Simulations for the Efficient Utilization of Stranded Methane Resources

ETHAN RYS
SPRING 2022

A thesis
submitted in partial fulfillment
of the requirements
for a baccalaureate degree
in Chemical Engineering
with honors in Chemical Engineering

Reviewed and approved* by the following:

Konstantinos Alexopoulos
Assistant Research Professor of Chemical Engineering
Thesis Supervisor

Themis Matsoukas
Professor of Chemical Engineering
Honors Adviser

* Electronic approvals are on file.

ABSTRACT

Non-oxidative methane coupling is the process of converting methane to C2 products through the C-C coupling of two methyl groups. While C2 products such as ethylene and ethane are valuable products as potential chemical feedstocks in the petrochemical industry, the process is limited by low yields of value-added products as the thermodynamic equilibrium favors heavy hydrocarbons and coke products under traditional continuous heating at high temperatures. Platinum has shown to be an appropriate catalyst for dissociating methane and adsorbing methyl groups to eventually form C2 products. Density functional theory (DFT) calculations are used to identify the reaction mechanism over a single platinum atom catalyst adsorbed on In_2O_3 (111), V_2O_5 (010), ZnO (100), and Ga_2O_3 (100) metal oxide supports. Pt/Ga_2O_3 (100) resulted in the lowest predicted apparent energy barrier to forming ethane as a result of stable intermediates along the reaction pathway. Controlling the time dependence of reactor temperature through dynamic heating profiles can alter the overall reactor performance. The ethylene yield on an FeC_2 on SiO_2 catalyst was significantly improved to 18% under a controlled heat pulse duration of 10 ms. The distribution of ethylene yield over various pulse durations and temperature ranges provides insight into reactor conditions that can best optimize the production of value-added products in methane conversion.

TABLE OF CONTENTS

LIST OF FIGURES

ACKNOWLEDGEMENTS

I want to thank Dr. Konstantinos Alexopoulos for welcoming me into his lab, spending countless hours explaining how to run calculations and interpret significant data, and all the time invested editing and revising my final Thesis. I would also like to thank Dr. Mike Janik for the constant support and advice on running DFT calculations as well as editing my draft and final Thesis. Additionally, I want to acknowledge and thank Gianna Caputo, Lucia Bruschi, and Jaehyung Lee for their contributing work in running DFT calculations to develop the studied catalytic cycles for platinum on four metal oxide surfaces. I also want to thank Dr. Themis Matsoukas for providing constant guidance throughout my four years of undergraduate, particularly in choosing which research path to take. Lastly, I want to thank my parents who have provided extraordinary support and guidance throughout the entire research and Thesis writing process that enabled me to provide my highest quality of work.

Chapter 1

Introduction

Natural gas is one of the most highly utilized sources of energy in the world, accounting for 24% of the global power generation.[1] However, methane, the main component of the fuel, has also drawn significant interest as a feedstock in the petrochemical industry following the discovery of shale gas reserves in the US.[2] Due to its economic and environmental advantage, methane catalytic conversion has been investigated as a strategy to synthesize C2 or higher hydrocarbons, syngas, methanol, and olefins.[2,3] As a result, the study of oxidative and non-oxidative coupling of methane has been analyzed as a potential mechanism to convert methane into value-added products; but these methods have not yet been scalable to industry due to yield limitations and separation costs.[4] Single-atom heterogenous catalysis with platinum has been studied as a potential approach to combat current shortcomings in research due to platinum's ability to activate the C-H bond of methane to light hydrocarbons.[5-8] Therein, the application of single-atom catalysts is explored to provide mechanistic pathways to higher yield of value-added products such as C2 hydrocarbons and light aromatics at higher conversions of methane.

In addition to catalytic chemistry, the heating profile during methane conversion can be further manipulated to take advantage of the early-forming C2 products and avoid the equilibrium preferred aromatics and coke products. While high selectivity to lower value C2 products such as acetylene can be obtained under high temperatures and short residence time, higher value products such as ethylene and ethane are more difficult to obtain a high yield due to high rates of reaction to heavier hydrocarbons.[9,10] As such, narrowly controlled heating profiles

present a potential advantage from traditional heating approaches such that value-added, initial forming of light hydrocarbons is maximized without allowing the reaction to proceed towards the undesirable equilibrium products.

Computational modeling techniques have enabled robust studies of catalytic performance without requiring the expenses and resources of laboratory experimentation. Density functional theory (DFT) calculations can be employed utilizing quantum mechanical first principles modeling techniques to identify transition states in a catalytic cycle. Through analysis of potential elementary steps and overall kinetics of a modeled catalytic cycle, the most efficient path to value-added products can be determined. We will evaluate the effectiveness of four metal oxide supports with an adsorbed platinum atom based on elementary reaction energetics for a catalytic cycle coupling methane molecules to form ethane and hydrogen.

Chemkin Pro software provides kinetic modeling tools that can be utilized to run first-principles-based reactor simulations for a variety of reactor types. This software allows detailed inputs from statistical thermodynamic calculations, gas-phase and surface kinetics, as well as transport data.[11] We will use this modeling tool to develop small scale reactors that allow rapid heating in a programmable way. Both continuous-stirred tank reactors (CSTR) and plug-flow reactors (PFR) are used as ideal reactor models to evaluate the product yield of methane conversion under various heating profiles. To maximize yield of value-added products while avoiding their rapid degradation, short heating pulses (10-100 ms) can be applied such that the residence time is sufficiently short enough to avoid reaction equilibrium.

In this study, we will examine the energetics of four metal oxide supports, In_2O_3 (111), V_2O_5 (010), ZnO (100), and Ga_2O_3 (100) with an adsorbed platinum atom in converting methane to ethane and hydrogen gas as seen in the overall reaction below.

Scheme 1: Methane conversion to ethane and hydrogen gas, where * denotes the metal surface with an adsorbed platinum atom.

$$2CH_4 + * \rightarrow C_2H_6 + H_2 + *$$

Additionally, the application of controlled heating ramp temperature profiles will be simulated to study the reaction products of non-oxidative methane conversion on the heterogeneous catalyst. The main objectives are to determine the reaction pathway over each Pt/metal oxide support system and evaluate the overall energetics as well as develop an optimized temperature profile for yielding value-added C2 products.

Chapter 2

Methods

2.1 Electronic Structure Calculations

Density functional theory was used to determine the transition states and intermediates for the catalytic cycles with an adsorbed platinum atom on each of the four metal oxide surfaces: In_2O_3(111), V_2O_5(010), ZnO(100), and Ga_2O_3(100). The Vienna Ab Initio Simulation Package (VASP) was used to perform the electronic structural calculations, operating on a plane-wave basis set and modeling ion-electron interactions with the projector augmented wave (PAW) method.[12] The exchange-correlation functional used for the calculations was the Perdew-Burke-Ernzerhof (PBE) exchange correlation. A cutoff energy of 450 eV was used for the plane-wave basis set. Structural calculations were iterated until the maximum forces of the modeled atoms converged to a minimum of 0.02 eV $Å^{-1}$. The k-space mesh sample used for the Pt on In_2O_3(111), V_2O_5(010), ZnO(100), and Ga_2O_3(100) was 2 × 2 × 1, 3 × 2 × 1, 4 × 2 × 1, and 4 × 2 ×1, respectively. To minimize dipole interactions, a sufficiently large vacuum layer of 15Å was chosen to separate the surface slabs. Transition states along the reaction pathway were identified using the nudged elastic band and dimer methods. The nudged elastic band calculation determines a starting point for the dimer calculations by attempting to connect the intended reactant and product.[13-15] An example of an identified transition state from Pt on In_2O_3 (111) can be found in Figure 20 in Appendix A.

2.2 Frequency Calculation

A normal mode analysis was determined using Partial Hessian Vibrational Analysis (PHVA) while fixing the metal surface atoms and allowing only the absorbates to be free to calculate the Hessian matrix.[13,16,17] Only harmonic frequencies were considered as the system was modeled as an ideal oscillator and avoids anharmonicities. An additional simplification made was to replace any low-lying frequency (<50 cm^{-1}) with a fixed value of cm^{-1} due to the inherent error in the calculation.[18-21]

2.3 Thermochemistry

The thermochemical and kinetic parameters are determined through application of statistical mechanics and transition state theory. The calculations are run in a Python multiscale thermochemistry toolbox (pMuTT) which converts ab-initio data to thermochemical properties such as Gibbs free energy, enthalpy, and entropy in addition to creating input files for kinetic modeling software.[22] The *ab initio* thermodynamics utilize statistical mechanics which considers the entropy contributions of equilibrium systems consisting of solid surfaces and gas-phase species to determine the free energy of each state.[23-30] The Gibbs free energy diagrams were determined at 500K, 1100K, and 1500K at standard pressure of 100 kPa.

2.4 Free Energy of Formation

The reference energy for the determined free energy profiles is based on the calculated free energy for the adsorbed platinum atom on the surface (G_*) and two gas-phase methane reactants (G_{CH_4}) as seen in equation 1.

$$G_{ref} = G_* + 2 * G_{CH_4} \quad (1)$$

The change in free energy from the reference state, for each possible intermediate and product species along the reaction path, is calculated from equation 2 where x and y represent the stoichiometric coefficients of the adsorbed species on the surface and m is the number of methane reactant molecules remaining in the gas-phase.

$$\Delta G_{C_xH_y^*} = G_{C_xH_y^*} + (m-2) * G_{CH_4} + \left(\frac{2-m-x}{2}\right) * G_{C_2H_6} + \left(\frac{2-m+3x-y}{2}\right) * G_{H_2} - G_* \quad (2)$$

2.5 Reactor Simulations

The reactor simulations were run with CHEMKIN, a software tool package which combines gas-phase, transport, and surface input data to allow for efficient modeling of chemical reactions in addition to modeling of the appropriate system of equations for the specified inputs.[31] CHEMKIN was primarily utilized in this study to model continuous-stirred tank reactor (CSTR) simulations. To model the catalytic reaction kinetics of methane conversion, the following rate expressions are defined:

$r = k(C_g)(C_*)^n$, for adsorption (3)

$r = k(C_s)^n$, for desorption (4)

$r = k\prod_i^n (C_s)_i$, for a surface reaction (5)

where r is the reaction rate (moles/cm^{2}s), C_g is the concentration of gaseous components (moles/cm^3), C_* is the surface concentration of free active sites (moles/cm^2), C_s is the surface concentration of a surface species (mol/cm^2), n is the reaction order, and k is the rate constant which must also be further specified.[32] The rate constants are based on the desorption/surface reaction and derived from transition state theory as seen below:

$$k_{des,surf} = \frac{A}{\sigma^{n-1}} \exp\left(-\frac{\Delta G^{\ddagger}}{RT}\right) \quad (6)$$

$$K = \exp\left(-\frac{\Delta G_{ads}}{RT}\right) \quad (7)$$

$$k_{ads} = k_{des} * K \quad (8)$$

where σ is the density of active sites (moles/cm^2), R is the ideal gas constant, T is the absolute temperature (K), $\Delta G^{\ddagger}$ represents the difference between the free energy of the transition state and initial reference species, ΔG_{ads} represents the free energy of adsorption, and A is the pre-exponential factor (s^{-1}).[31]

To emulate a transient reactor operation, a CSTR model was chosen for this study with a temporal profile instead of a plug flow reactor model that allows a spatial variation of the temperature along its axial position. In addition to gas-phase, thermodynamics, and surface input files, the simulation required inputs were temperature, pressure, volume, residence time, mass flowrate, catalyst internal surface area, inlet mole fraction of reactants. For all simulations, a pressure of 1 atm, volume of 7.3 x10^{-3} cm^3, catalyst internal area of 0.13 cm^2, and mass flow rate of 6.55x10^{-5} g*s^{-1} was used. The site time, defined as the number of active sites in moles per inlet flow rate of methane, over the platinum catalyst on each metal oxide support was run at 1.26x10^{-4} mol Pt*s/mol CH_4.[18] The residence time and temperature varies based on the heating profile.

Due to the limitation of recreating computational conditions in a laboratory setting, only the rise from a lower temperature to the max pulse temperature was considered to avoid results that could not further be reasonably analyzed experimentally. Additionally, gas-phase kinetics together with their thermodynamic input files were added in all simulations including the ones with a Pt heterogeneous catalyst and were taken from a previous study evaluating high temperature combustion of hydrocarbon fuels.[33] The data from this study was determined to be suitable as it allows for simulations to be conducted under the higher temperatures that are studied under the investigated heating ramp temperature profiles.

Chapter 3

Results and Discussion

We will first compare the energetics of non-oxidative methane coupling to ethane on Pt on the four metal oxide supports and examine each's ability to complete a catalytic cycle. Additionally, we will evaluate the effect of applying various heating ramp temperature profiles during the process of methane conversion in attempt to maximize the yield of C2-products. In each section, the Pt catalyst will be compared with an iron-carbide catalyst from previous studies that has exhibited success in the selective conversion of methane to ethylene.[18] Section 3.1 will consider the reaction progress and free energy of the coupling reaction on Pt for each support. Section 3.2 will shift to examining reactor simulations under various heat ramp temperature profiles to compare how the product distribution can be manipulated by pulse duration and peak temperature.

3.1 Platinum Catalyst on In_2O_3 (111), V_2O_5 (010), Ga_2O_3 (100), and ZnO (100) Surfaces

Figure 1 highlights the four different metal oxide supports which were introduced in this study. The binding energy of platinum on each of these surfaces was found to be 351, 469, 165, and 468 kJ/mol for In_2O_3 (111), V_2O_5 (010), Ga_2O_3 (100), and ZnO (100), respectively. Figure 1 more clearly visualizes the Pt atom on the different oxide supports and shows Pt coordinating to two surface oxygens on In_2O_3, four surface oxygens on both V_2O_5 and Ga_2O_3, and no surface oxygens on ZnO due to the presence of an oxygen vacancy.

Figure 1 The top left image is Pt adsorbed on In_2O_3 (111) support, top right is Pt adsorbed on V_2O_5 (010) support, bottom left is Pt adsorbed on ZnO (100), and bottom right is Pt adsorbed on Ga_2O_3 (100) support

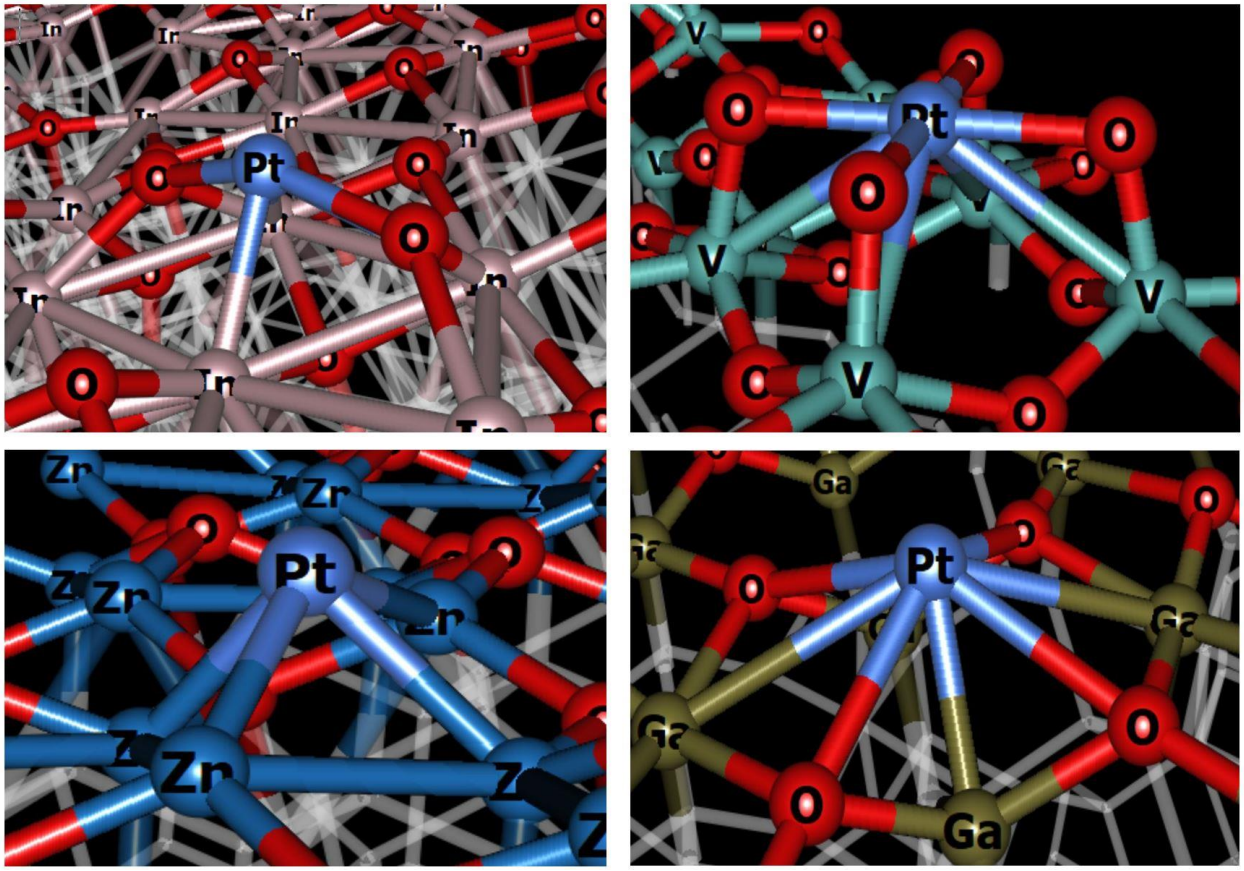

The four studied metal oxide supports follow similar pathways in converting methane into ethane. Figure 2 highlights the catalytic cycle for ethane production on In_2O_3 as both platinum and the neighboring oxygen atoms of the support are involved in the process. The spillover of hydrogen onto oxygen promotes steric proximity of the two adsorbed methyl groups on platinum, allowing for the two groups to readily interact to form ethane and desorb from the surface. However, the strong adsorption of hydrogen onto the neighboring oxygen atoms leads to a rather stable intermediate D, which limits the ability of the catalyst to complete a full cycle, as visible in energetics found in Figure 3.

Figure 2 In_2O_3 (111) ethane production cycle

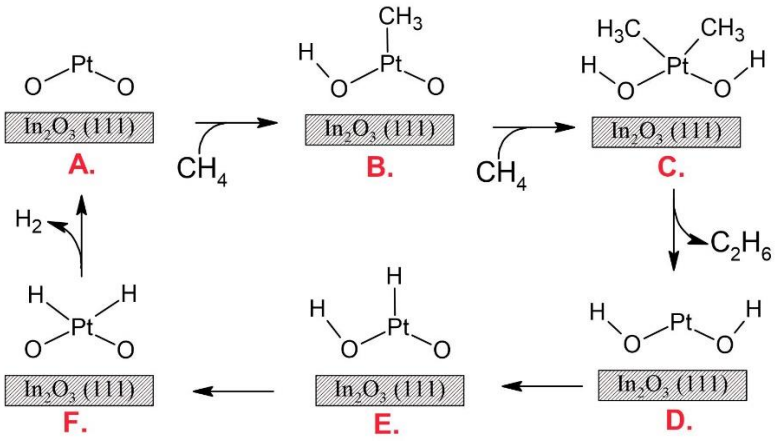

Figure 3 Methane coupling free energy diagram over a Pt/In_2O_3 catalyst at 1100K and 100 kPa

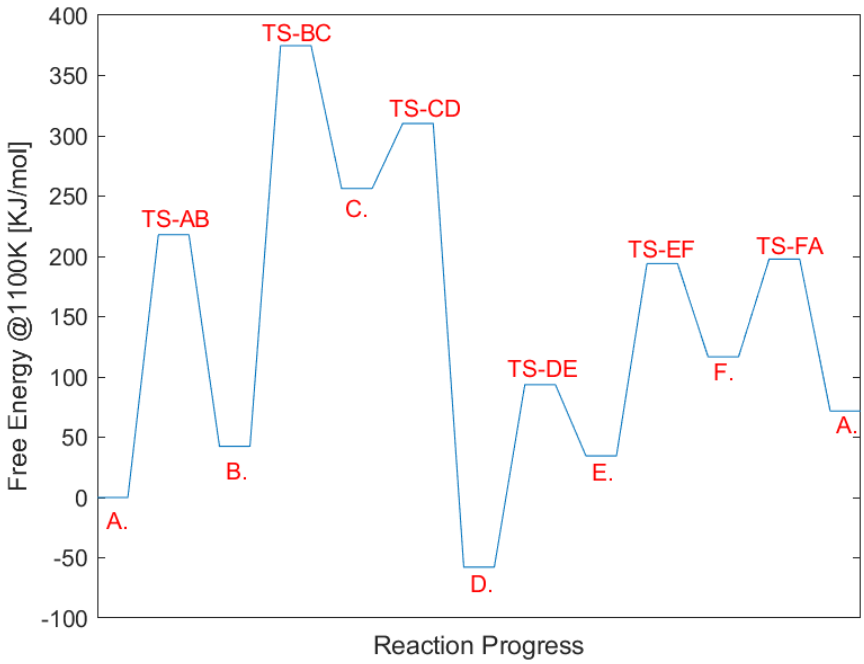

Next, the catalytic cycle for platinum on V_2O_5 (010) is illustrated in Figure 4. Several molecular shifts were required in this process as in steps H. to I. and K. to L. in order for the desired products to be formed. Because of the high oxygen coordination around the Pt atom

(namely, 4 oxygen atoms), this fully oxidized vanadium support was found to be ineffective in forming ethane. Overall, the proposed pathway followed a consecutive and significant increase in free energy that was not found to be preferable towards the desired products formation.

Figure 4 V_2O_5 (010) ethane production cycle

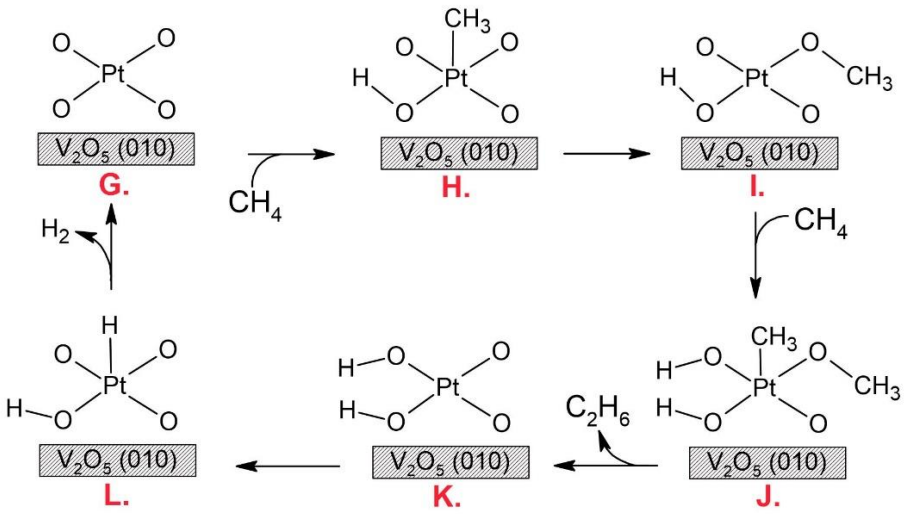

Figure 5 Methane coupling free energy diagram over a Pt/V_2O_5 catalyst at 1100K and 100 kPa

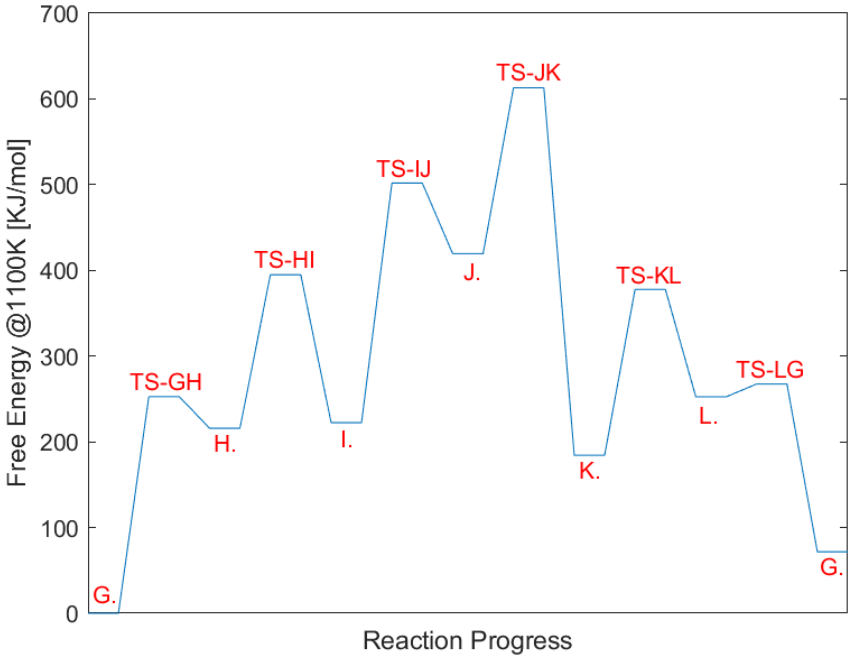

In the case of ZnO, the Pt atom sits in an oxygen vacancy and the absence of nearby oxygen atoms (see Figure 1) forces the adsorbates to stay on on the platinum atom, limiting the amount of reaction steps (see Figure 6). However, the free energy of intermediate and transition states become less favorable for this catalytic cycle (see Figure 7) in comparison to the In_2O_3 cycle.

Figure 6 ZnO (100) ethane conversion cycle

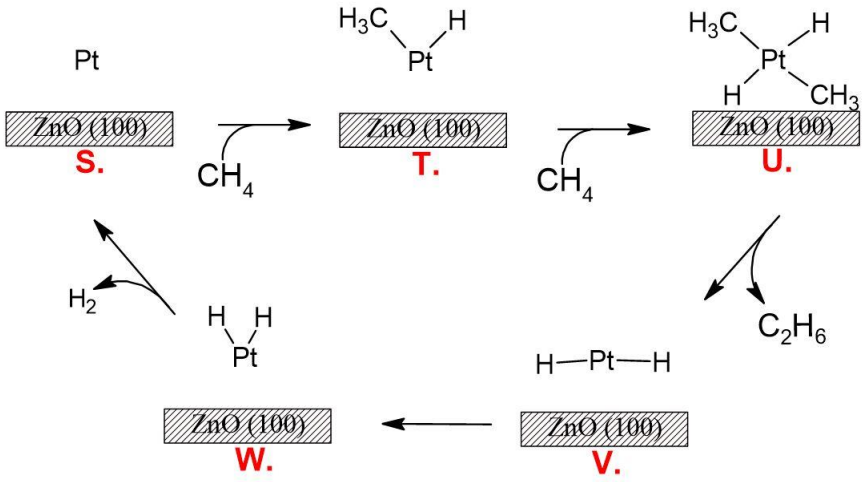

Figure 7 Methane coupling free energy diagram over a Pt/ZnO catalyst at 1100K and 100 kPa

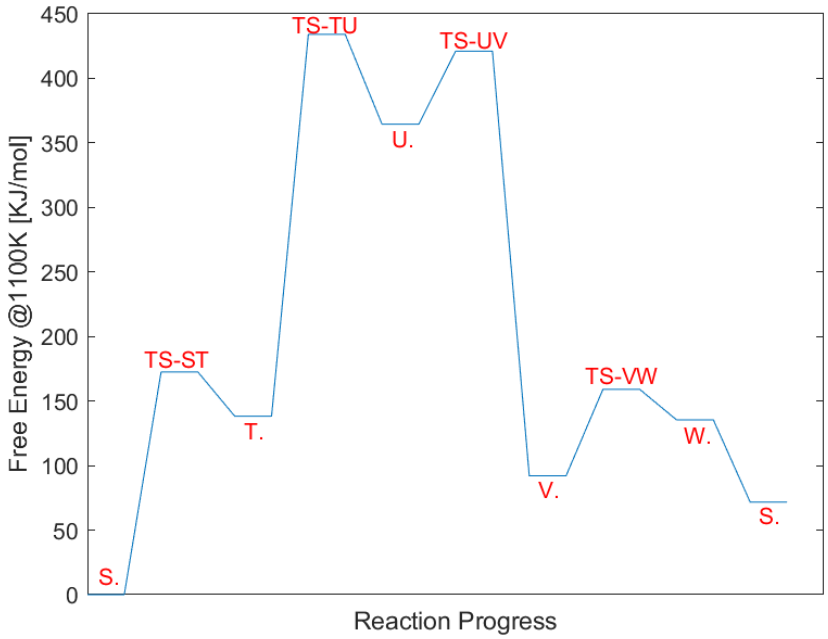

Finally considering Ga_2O_3 the proposed mechanism to ethane production was found to be the most effective of the four considered metal oxide supports. Comparing this mechanism to V_2O_5 which has a similar active site, there a few key differences. First is the adsorption of the methyl groups as they both remain on platinum allowing for a closer proximity to form ethane. Secondly, the hydrogen dissociated from the second adsorbed methyl does not transition to a neighboring oxygen which avoids the system from being over-stabilized once ethane desorbs. Lastly, after C-C coupling, an additional step is required for ethane desorption due to the interaction of ethane with the active site. The overall mechanism is shown in Figure 8.

Figure 8 Ga_2O_3 ethane production cycle

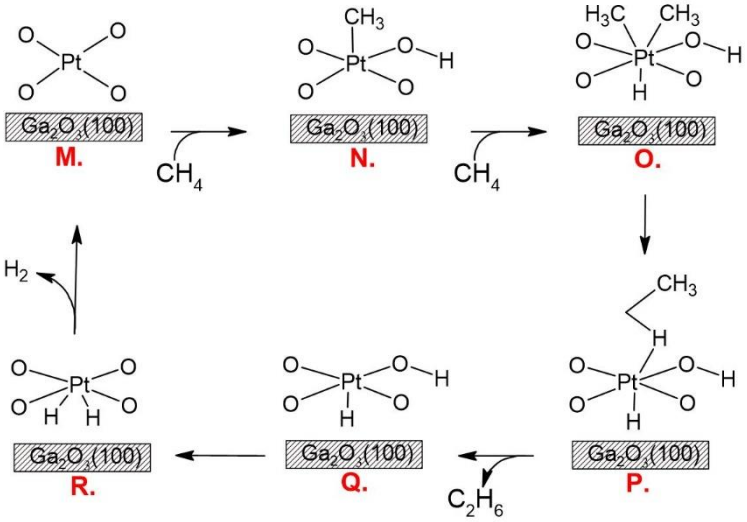

Figure 9 Methane coupling free energy diagram over a Pt/Ga_2O_3 catalyst at 1100K and 100 kPa

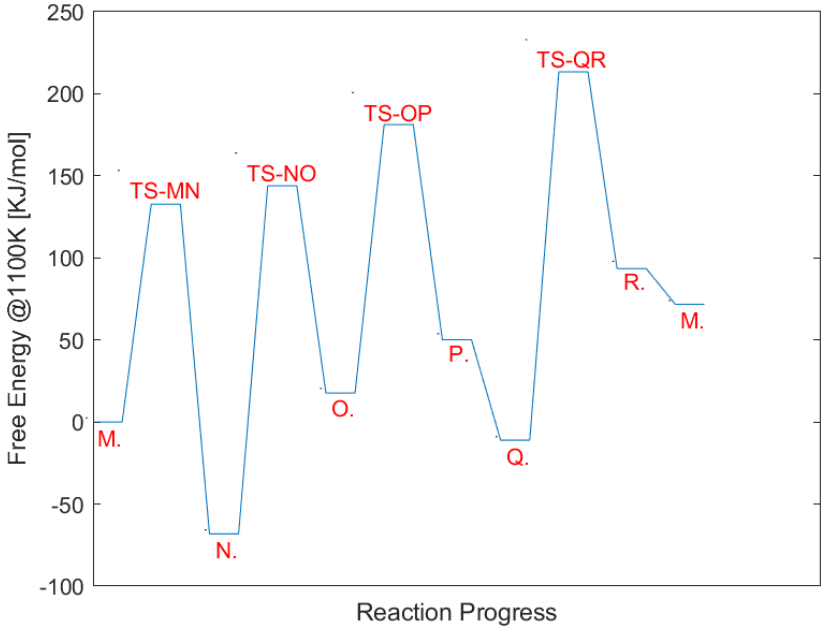

Figure 10 shows the free energy diagrams from the non-oxidative coupling of methane on the In_2O_3, V_2O_5, Ga_2O_3, and ZnO metal oxide supports with an adsorbed Pt atom. The free energy of the endothermic coupling reaction of two methane molecules to ethane and H_2 was found to be 72 kJ/mol at 1100K.

Figure 10 Methane coupling to ethane free energy diagram over a Pt/In_2O_3 (111), Pt/V_2O_5 (010), and Pt/Ga_2O_3 (100), Pt/ZnO (100) catalyst at 1100K and 100 kPa

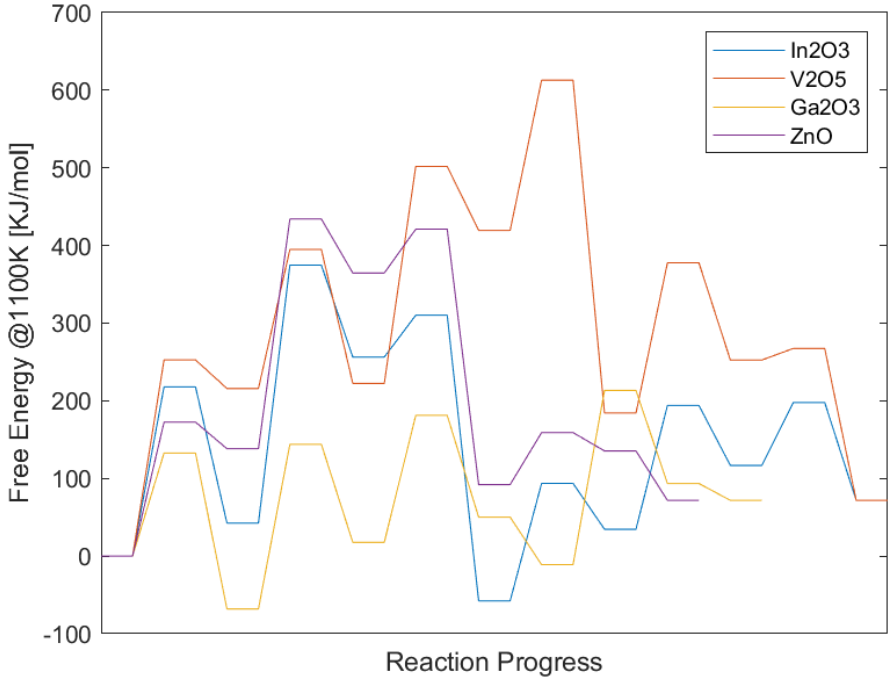

To evaluate the energy span for each catalytic cycle, application of the Murdoch procedure was considered.[34] The procedure segments portions of the reaction profile based on the energy of intermediates in comparison to the reactants, only constituting a new reaction segment when an intermediate has a lower free energy than the reactants or previous intermediate. The reaction segment with the largest difference between the reactant or intermediate that begins the reaction segment and the highest transition state in that segment would dictate the energy span of the catalytic cycle. An example of this procedure is shown in Figure 11, which was applied to Pt on In_2O_3. For this cycle, there is only one intermediate with lower energy than the initial reactants, therefore there are only two segments of the reaction profile to consider, taking the difference between TS-BC and reactant A. as well as TS-FA and intermediate D. with the larger of the two differences determining the energy span.

Figure 11 Energy span determination using the Murdoch procedure for methane coupling on Pt/In_2O_3 (111) catalyst

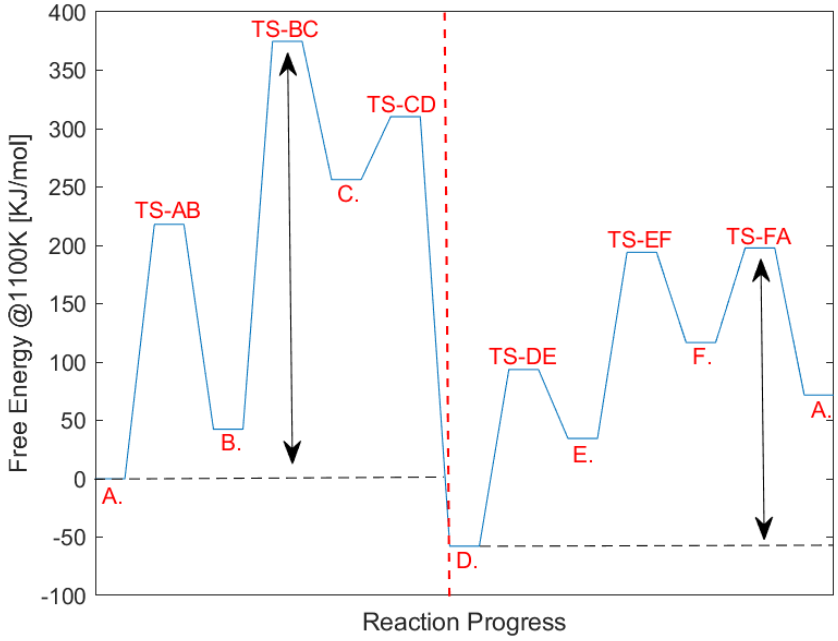

The determined energy span for Pt on In_2O_3 at 1100K was found to be 375 kJ/mol. The same procedure was applied to the platinum catalyst on each of the four metal oxide supports and the results are available in Figure 12 for different temperatures. Based on the assessment of the energy spans at 1100K, Ga_2O_3 appears to have the most promising energetics with the lowest apparent energy span of 282 kJ/mol.

It is also interesting to consider how the energetics of the catalysts change with temperature as the entropic contributions become more significant. As temperature increases, the significance of entropy losses makes surface intermediates and transition states less stable compared to the gas-phase reactants, thus leading to an increase in the energy span for each of catalyst with respect to temperature. Interestingly, however, the energy span increases faster with temperature on some supports compared to others (see Figure 12). The support whose energy span is least influenced by temperature, namely Ga_2O_3, is found to be the most promising one

over the complete temperature range. Figure 13 depicts the energy diagram of platinum on Ga_2O_3 as the temperature rises, showcasing how the energy span is kept relatively constant over a wide range of temperature.

Figure 12 Energy span for platinum catalyst on In_2O_3, V_2O_5, ZnO, and Ga_2O_3 as a function of temperature at 100 kPa

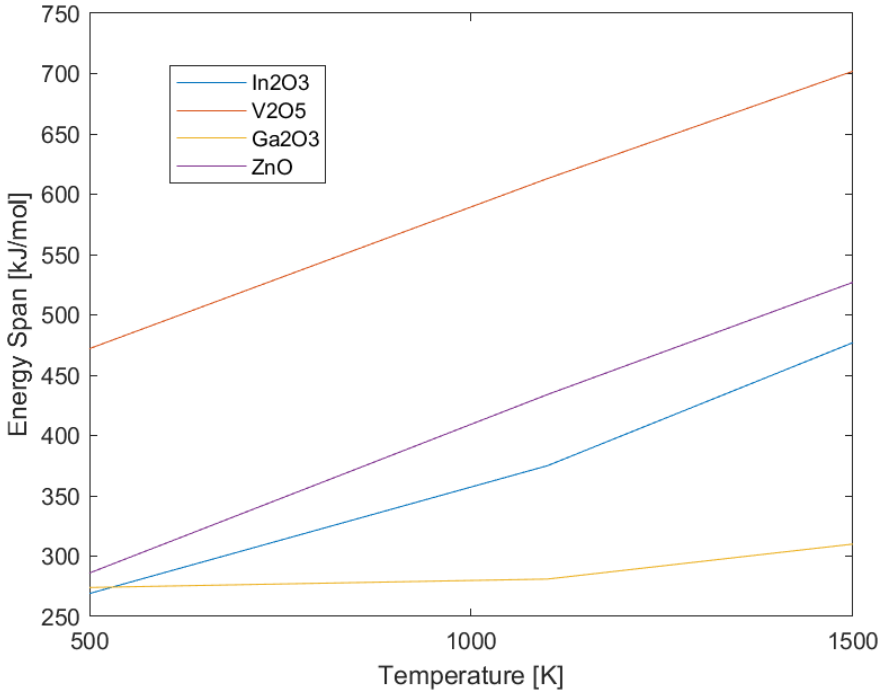

Figure 13 Pt/Ga_2O_3 catalyst free energy diagram for methane coupling at 500K, 1100K and 1500K. All three energetics determined at 100 kPa

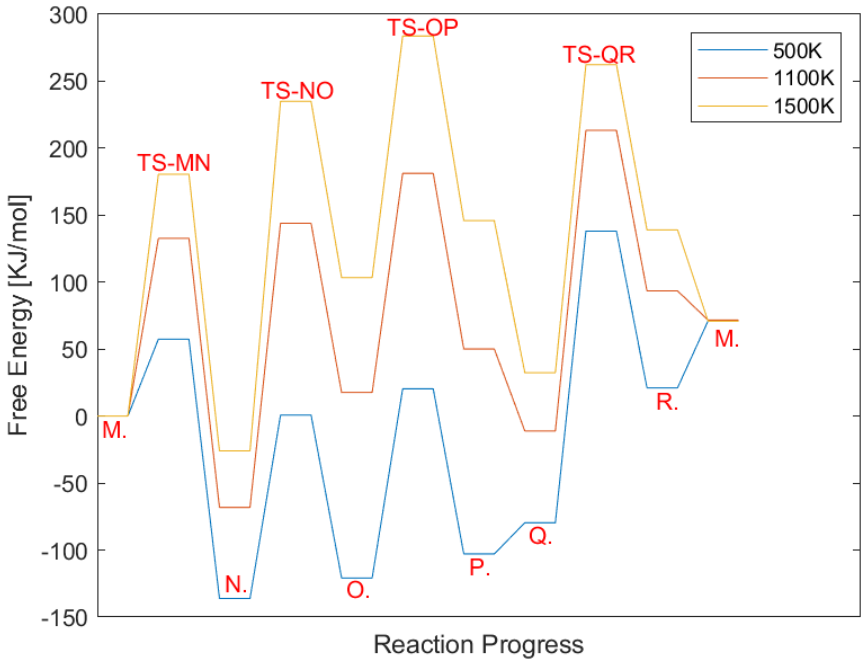

At 500K, the limiting step considered in the energy span is between intermediate N and the transition state at TS-QR. As temperature reaches to 1500K, the limiting transition state changes from TS-QR to TS-OP, shifting from the reserve spillover of hydrogen to the C-C coupling on the Pt atom. The main consideration for this change in rate determining steps is driven by entropic factors that are linked to ethane desorption from the surface. At low temperatures, ethane adsorption is preferable to ethane desorbing into the gas-phase as visible in the slight increase in free energy between the two steps. However, as the temperature rises and the entropy contribution to the free energy begins to dominate, ethane becomes more favorable in the gas-phase, which accounts for the desorption of ethane having a lower energy than the adsorbed ethane after exceeding 500K. Similarly, this also leads to a significant destabilization of TS-OP (which consists of two adsorbed methyl groups) with respect to gas-phase ethane at higher temperatures.

3.2 Heat Ramp Simulations

Due to the preference of heavy hydrocarbons and coke products formation at equilibrium conditions seen in methane combustion at high temperatures, a controlled heating profile limiting the residence time at high temperatures is explored as a potential solution to yield higher-value products such as ethane and ethylene. In order to accomplish a high selectivity of these products with a sufficient conversion of methane, various heating ramps where considered to maximize both of these considerations. A temperature ramp profile was applied to methane on each of the four metal oxide supports and Figure 14 depicts four different heat pulses applied with a duration of 50 ms, 100 ms, 200 ms, and 300 ms.

Figure 14 Temperature profiles during methane conversion on Pt catalyst. Data was only collected during the duration of the heat pulse

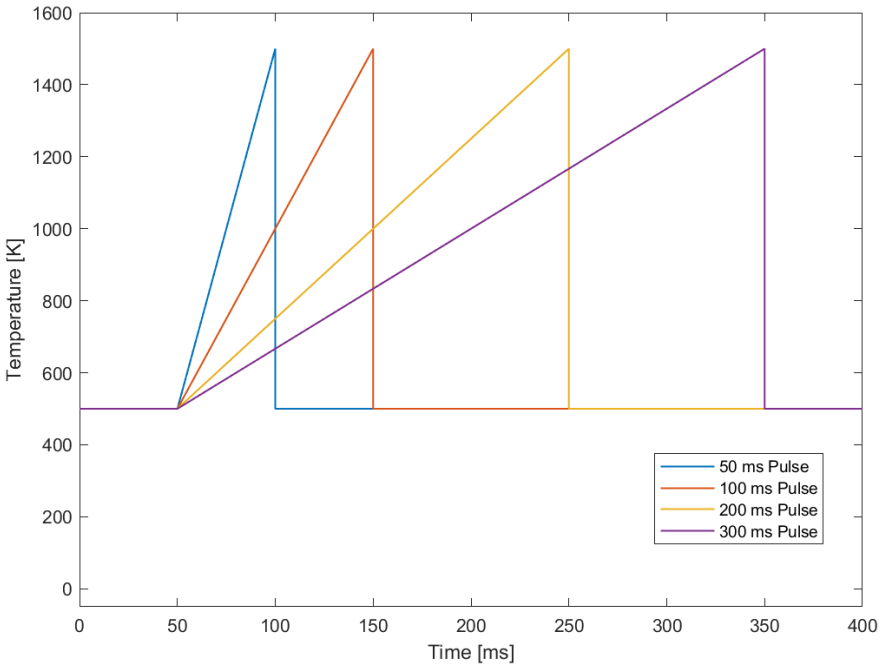

Ultimately, using the heating profiles did not have any impact on kinetics and reaction products for platinum on In_2O_3, V_2O_5, and ZnO, however, the Ga_2O_3 did have interesting results.

Figure 15 compares the conversion of methane under a 100 ms heating ramp temperature profile when the catalyst is present and removed. While the catalyst was effective in increasing the overall conversion from 1% to 11% in only 100 ms, the yield of value-added products was not seen to be significant as seen in Figure 16**.** This was mainly attributed to the lack catalytic pathways since the catalyst was modeled to yield only ethane which reaches a selectivity of 97%, however, quickly reverts to the equilibrium dominated products and degrades in higher hydrocarbons. It would be worth considering to model additional pathways to other value-added products such as ethylene.

Figure 15 Methane conversion with Pt on Ga_2O_3 present (solid blue) and absent (dashed blue) during 100 ms heat ramp from 500K to 1500K

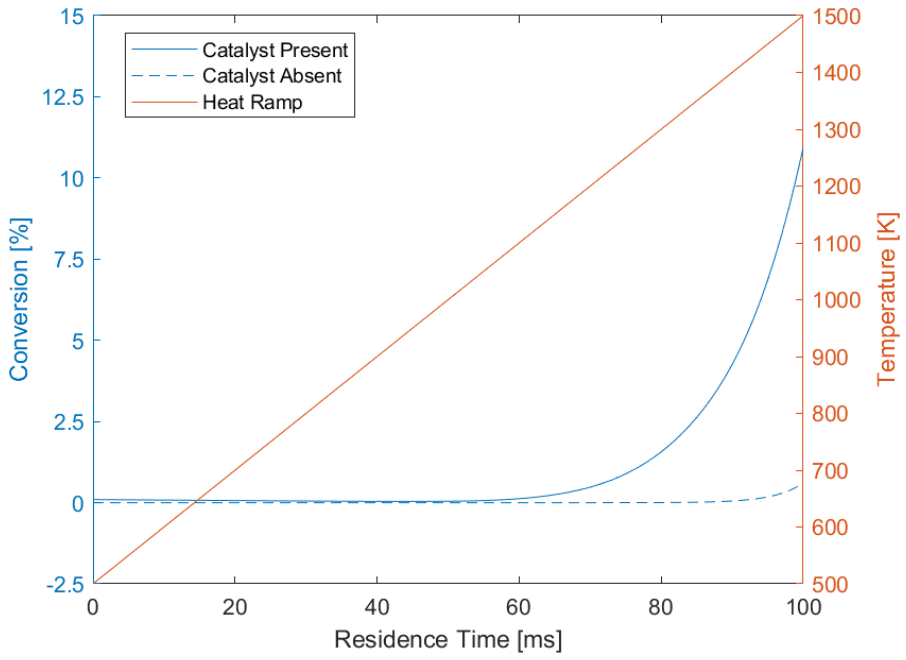

Figure 16 Selectivity and Yield of ethylene and ethane over 100 ms heat ramp. The solid lines represent the selectivity of the products and the dashed lines represents the yield of the products

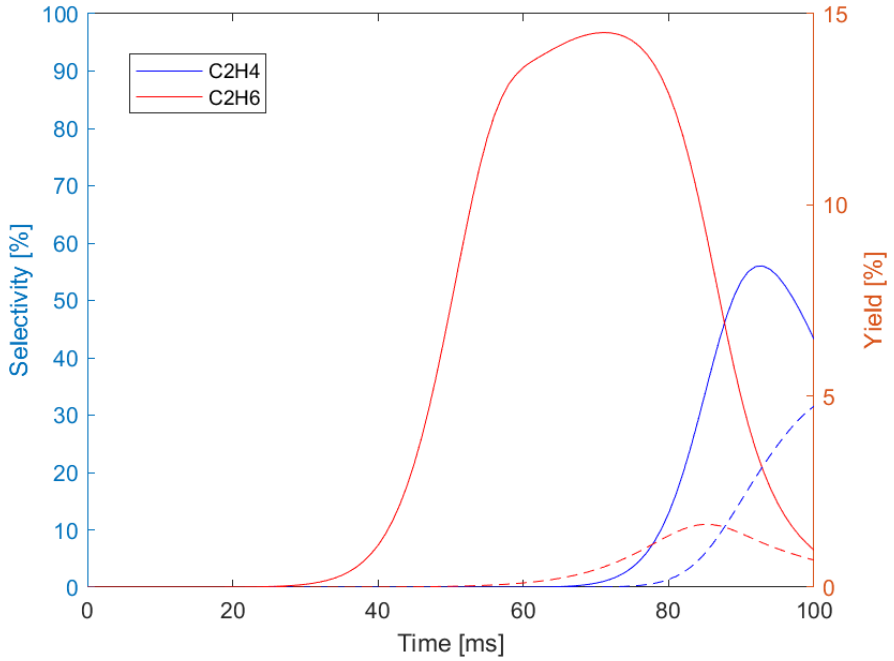

The effect of a heat ramp temperature profile was further considered on a more developed heterogenous catalyst model, namely FeC_2 on SiO_2 from Toraman et al.[18] In comparison to the single pathway that was modeled in the four previously discussed catalysts, FeC_2 on SiO_2 was found to be highly selective towards ethylene. Therefore, several temperature profiles at higher temperatures were applied in the present study in an attempt to increase the overall methane conversion with ethylene being the target product.

The applied temperature ramps included a 400K increase from a initial to final temperature over the course of 10 ms, 20 ms, 50 ms, 75 ms, and 100 ms. Figure 17 highlights each of these pulse durations that were applied at a starting temperature of 1100K. The starting temperature for each pulse varied between 1100K, 1150K, 1200K, and 1250K as shown in Figure 18 for a fixed pulse duration (50 ms) and this was repeated for the different pulse

durations (10, 25, 75, 100 ms). Additionally, data was only collected from the initial point of a temperature increase until the temperature reaches its highest temperature.

Figure 17 Heat ramp temperature profiles for FeC_2 catalyst on SiO_2. The figure highlights all the different heat ramp durations considered at a starting temperature of 1100K and ending temperature of 1500K.

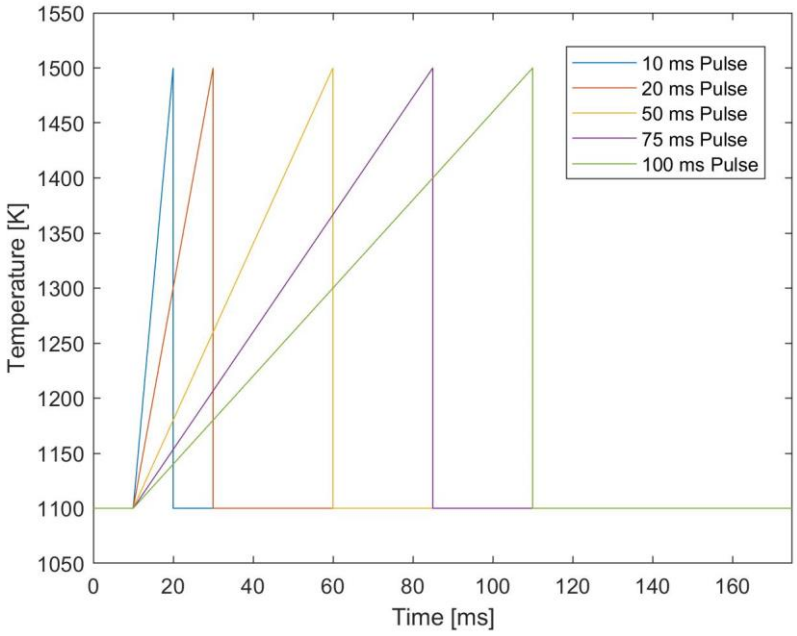

Figure 18 Heat ramp temperature profiles for FeC_2 catalyst on SiO_2. The pulse length for each of the four initial considered starting temperatures is 50 ms.

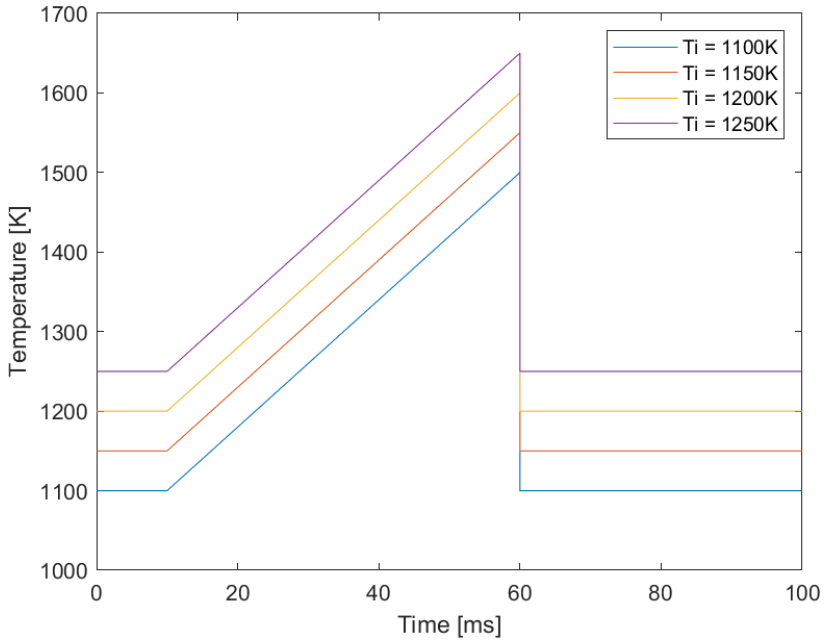

The results of these simulations are visualized in Figure 19 which highlights the yield of ethylene at each pulse duration and end temperature of the pulse. Ultimately, the maximum yield of ethylene determined was 18% which underwent a 10 ms heating ramp starting at 1250K and ending at 1650K. The distribution of results indicates that shorter pulses at higher temperatures were most effective in producing high yields of ethylene. This was attributed to the higher average temperature of the pulse which increases methane conversion to ethylene and a short residence time that does not extend beyond the early induction period of the reaction that favors C2-C3 product formation. Longer pulse durations at higher temperatures exceed this initial reaction timescale and rapidly begin to degrade the initially formed C2 products into heavier hydrocarbons which are preferred at equilibrium.

Figure 19 Map of C2H4 yields at each pulse duration and temperature profile analyzed. The y-axis accounts for the final temperature of the heating ramp, therefore the initial temperature is 400K lower at each point.

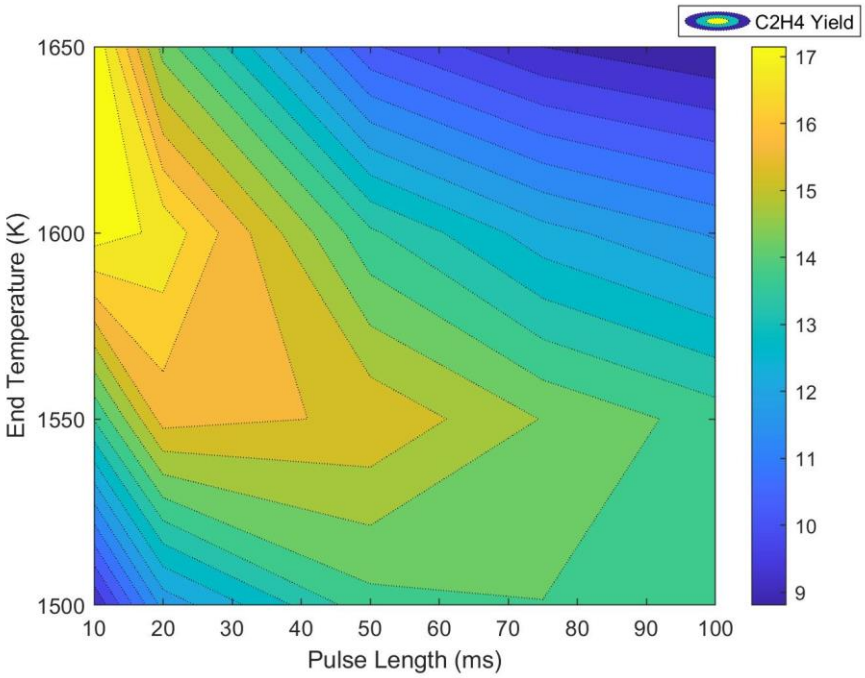

Chapter 4

Summary and Conclusion

We studied non-oxidative methane coupling to form ethane on In_2O_3 (111), V_2O_5 (010), ZnO (100), and Ga_2O_3 (100) metal oxide support with an adsorbed platinum atom. Based on the energetics from DFT calculations and application of the Murdoch procedure to identify the rate determining steps of each mechanism and the resulting energy span, platinum adsorbed on Ga_2O_3 (100) had the lowest energy span and was the only catalyst that was able to form significant amounts of ethane.

Furthermore, prior work on non-oxidative coupling of methane over a highly selective catalyst has highlighted the importance of quenching the gas-phase chemistry that is omnipresent at high temperatures in order to avoid significant selectivity loss.[18] Therefore, controlled heat ramp temperature profiles were studied under short residence times from 10-300 ms. Ultimately, an applied heating ramp temperature profile from 1250K to 1650K over a 10 ms duration was determined to significantly improve the yield of ethylene to 18% on the silica supported FeC_2 catalyst.

Appendix A

Supporting Information

Figure 20 Transition state identified for ethane formation on the Pt/In_2O_3 (111) catalyst where Pt is pink, oxygen is red, hydrogen is white, and carbon is orange

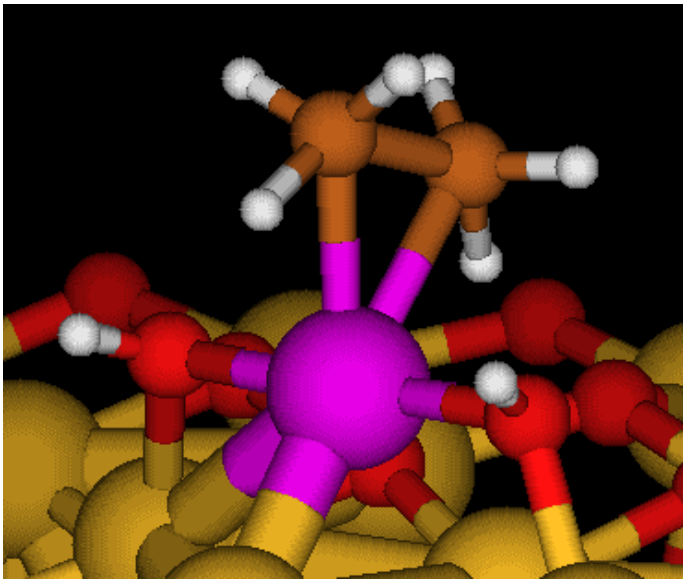

BIBLIOGRAPHY

1. IEA (2021), *Natural Gas-Fired Power*, IEA, Paris https://www.iea.org/reports/natural-gas-fired-power

2. Thyssen, V. V., Vilela, V. B., de Florio, D. Z., Ferlauto, A. S., & Fonseca, F. C. (2022). Direct conversion of methane to C2 hydrocarbons in solid-state membrane reactors at high temperatures. *Chemical Reviews*, *122*(3), 3966–3995. https://doi.org/10.1021/acs.chemrev.1c00447

3. Guo, X.; Fang, G.; Li, G.; Ma, H.; Fan, H.; Yu, L.; Ma, C.; Wu, X.; Deng, D.; Wei, M.; Tan, D.; Si, R.; Zhang, S.; Li, J.; Sun, L.; Tang, Z.; Pan, X.; Bao, X. Direct, Nonoxidative Conversion of Methane to Ethylene, Aromatics, and Hydrogen. *Science* **2014**, *344* (6184), 616–619. https://doi.org/10.1126/science.1253150.

4. Stünkel, S.; Bittig, K.; Godini, H.-R.; Jaso, S.; Martini, W.; Arellano-Garcia, H.; Wozny, G. Process Development in a Miniplant Scale - a Multilevel - Multiscale PSE Approach for Developing an Improved Oxidative Coupling of Methane Process. *Computer Aided Chemical Engineering* **2012**, *31*, 1692–1696. https://doi.org/10.1016/b978-0-444-59506-5.50169-3.

5. Xie, P.; Pu, T.; Nie, A.; Hwang, S.; Purdy, S. C.; Yu, W.; Su, D.; Miller, J. T.; Wang, C. Nanoceria-Supported Single-Atom Platinum Catalysts for Direct Methane Conversion. *ACS Catalysis* **2018**, *8* (5), 4044–4048. https://doi.org/10.1021/acscatal.8b00004.

6. Chin, Y. H.; Buda, C.; Neurock, M.; Iglesia, E., Reactivity of Chemisorbed Oxygen Atoms and Their Catalytic Consequences during CH4-O-2 Catalysis on Supported Pt Clusters. J. Am. Chem. Soc. 2011, 133, 15958-15978.

7. Sattler, J. J. H. B.; Gonzalez-Jimenez, I. D.; Luo, L.; Stears, B. A.; Malek, A.; Barton, D. G.; Kilos, B. A.; Kaminsky, M. P.; Verhoeven, T. W. G. M.; Koers, E. J.; Baldus, M.; Weckhuysen, B. M., Platinum-Promoted Ga/Al2O3 as Highly Active, Selective, and Stable Catalyst for the Dehydrogenation of Propane. Angew. Chem. Int. Ed. 2014, 53, 9251-9256.

8. Vajda, S.; Pellin, M. J.; Greeley, J. P.; Marshall, C. L.; Curtiss, L. A.; Ballentine, G. A.; Elam, J. W.; Catillon-Mucherie, S.; Redfern, P. C.; Mehmood, F.; Zapol, P., Subnanometre platinum clusters as highly active and selective catalysts for the oxidative dehydrogenation of propane. Nat. Mater. 2009, 8, 213-216.

9. Huang, K.; Miller, J. B.; Huber, G. W.; Dumesic, J. A.; Maravelias, C. T. A General Framework for the Evaluation of Direct Nonoxidative Methane Conversion Strategies. *Joule* **2018**, *2* (2), 349–365. https://doi.org/10.1016/j.joule.2018.01.001.

10. Holmen, A.; Olsvik, O.; Rokstad, O. A. Pyrolysis of Natural Gas: Chemistry and Process Concepts. *Fuel Processing Technology* **1995**, *42* (2-3), 249–267. https://doi.org/10.1016/0378-3820(94)00109-7.

11. Kee, R.; Rupley, F.; Miller, J. Chemkin-II: A Fortran Chemical Kinetics Package for the Analysis of Gas-Phase Chemical Kinetics. **1989**. https://doi.org/10.2172/5681118.

12. Hafner, J. Ab-Initio Simulations of Materials Using VASP: Density-Functional Theory and Beyond. *Journal of Computational Chemistry* **2008**, *29* (13), 2044–2078. https://doi.org/10.1002/jcc.21057.

13. Alexopoulos, K.; Vlachos, D. G. Surface Chemistry Dictates Stability and Oxidation State of Supported Single Metal Catalyst Atoms. *Chemical Science* **2020**, *11* (6), 1469–1477. https://doi.org/10.1039/c9sc05944j.

14. Henkelman, G.; Jónsson, H. Improved Tangent Estimate in the Nudged Elastic Band Method for Finding Minimum Energy Paths and Saddle Points. *The Journal of Chemical Physics* **2000**, *113* (22), 9978–9985. https://doi.org/10.1063/1.1323224.

15. Henkelman, G.; Jónsson, H. A Dimer Method for Finding Saddle Points on High Dimensional Potential Surfaces Using Only First Derivatives. *The Journal of Chemical Physics* **1999**, *111* (15), 7010–7022. https://doi.org/10.1063/1.480097.

16. Canduela-Rodriguez, G.; Sabbe, M. K.; Reyniers, M.-F.; Joly, J.-F.; Marin, G. B. Periodic DFT Study of Benzene Adsorption on Pd(100) and Pd(110) at Medium and Saturation Coverage. *The Journal of Physical Chemistry C* **2014**, *118* (37), 21483–21499. https://doi.org/10.1021/jp506158c.

17. De Moor, B. A.; Ghysels, A.; Reyniers, M.-F.; Van Speybroeck, V.; Waroquier, M.; Marin, G. B. Normal Mode Analysis in Zeolites: Toward an Efficient Calculation of Adsorption Entropies. *Journal of Chemical Theory and Computation* **2011**, *7* (4), 1090–1101. https://doi.org/10.1021/ct1005505.

18. Toraman, H. E.; Alexopoulos, K.; Oh, S. C.; Cheng, S.; Liu, D.; Vlachos, D. G. Ethylene Production by Direct Conversion of Methane over Isolated Single Active Centers. *Chemical Engineering Journal* **2021**, *420*, 130493. https://doi.org/10.1016/j.cej.2021.130493.

19. Alexopoulos, K.; John, M.; Van der Borght, K.; Galvita, V.; Reyniers, M.-F.; Marin, G. B. DFT-Based Microkinetic Modeling of Ethanol Dehydration in H-ZSM-5. *Journal of Catalysis* **2016**, *339*, 173–185. https://doi.org/10.1016/j.jcat.2016.04.020.

20. Canduela-Rodriguez, G.; Sabbe, M. K.; Reyniers, M.-F.; Joly, J.-F.; Marin, G. B. Thermodynamic Study of Benzene and Hydrogen Coadsorption on Pd(111). *Phys. Chem. Chem. Phys.* **2014**, *16* (43), 23754–23768. https://doi.org/10.1039/c4cp02991g.

21. De Moor, B. A.; Reyniers, M.-F.; Marin, G. B. Physisorption and Chemisorption of Alkanes and Alkenes in H-FAU: A Combined Ab Initio–Statistical Thermodynamics Study. *Physical Chemistry Chemical Physics* **2009**, *11* (16), 2939–2958. https://doi.org/10.1039/b819435c.

22. Lym, J.; Wittreich, G. R.; Vlachos, D. G. A Python Multiscale Thermochemistry Toolbox (pMuTT) for Thermochemical and Kinetic Parameter Estimation. *Computer Physics Communications* **2020**, *247*, 106864. https://doi.org/10.1016/j.cpc.2019.106864.

23. Senftle, T. P.; van Duin, A. C. T.; Janik, M. J. *Computational Catalysis*; Asthagiri, A., Janik, M. J., Eds.; Royal Society of Chemistry: Cambridge, 2013; pp. 157–191. https://doi.org/10.1039/9781849734905.

24. Reuter, K.; Frenkel, D.; Scheffler, M. The Steady State of Heterogeneous Catalysis, Studied by First-Principles Statistical Mechanics. *Physical Review Letters* **2004**, *93* (11). https://doi.org/10.1103/physrevlett.93.116105.

25. Rogal, J.; Reuter, K.; Scheffler, M. Thermodynamic Stability of PdO Surfaces. *Physical Review B* **2004**, *69* (7). https://doi.org/10.1103/physrevb.69.075421.

26. Sholl, D. S.; Steckel, J. A. *Density Functional Theory: A Practical Introduction*; John Wiley & Sons, Inc, 2009; pp. 1–233.

27. Stampfl, C. Surface Processes and Phase Transitions from Ab Initio Atomistic Thermodynamics and Statistical Mechanics. *Catalysis Today* **2005**, *105* (1), 17–35. https://doi.org/10.1016/j.cattod.2005.04.015.

28. Reuter, K.; Scheffler, M. Composition, Structure, and Stability OfRuO2(110)as a Function of Oxygen Pressure. *Physical Review B* **2001**, *65* (3). https://doi.org/10.1103/physrevb.65.035406.

29. Reuter, K.; Scheffler, M. Composition and Structure of TheRuO2(110)Surface in AnO2and CO Environment: Implications for the Catalytic Formation Of CO2. *Physical Review B* **2003**, *68* (4). https://doi.org/10.1103/physrevb.68.045407.

30. Reuter, K.; Scheffler, M. First-Principles Atomistic Thermodynamics for Oxidation Catalysis: Surface Phase Diagrams and Catalytically Interesting Regions. *Physical Review Letters* **2003**, *90* (4). https://doi.org/10.1103/physrevlett.90.046103

31. Kee, R. J.; Rupley, F. M.; Miller, J. A.; Coltrin, M. E.; Grcar, J. F.; Meeks, E.; Moffat, H. K.; Lutz, A. E.; Dixon-Lewis, G.; Smooke, M. D.; Evans, G. H.; Larson, R. S.; Mitchell, R. E.; Petzold, L. R.; Reynolds, W. C.; Caracotsios, M.; Stewart, W. E.; Glarborg, P.; Wang, C.;

Adigun, O. *The CHEMKIN Thermodynamic Database*; Reactor Design, Inc.: San Deigo, CA, 2000.

32. Hansgen, D. A. (2011). *Rational catalyst design for the ammonia decomposition reaction* (Order No. 3473687). Available from ProQuest Dissertations & Theses Global; ProQuest One Academic. (896363838). Retrieved from https://www.proquest.com/dissertations-theses/rational-catalyst-design-ammonia-decomposition/docview/896363838/se-2?accountid=147094

33. Blanquart, G.; Pepiot-Desjardins, P.; Pitsch, H. Chemical Mechanism for High Temperature Combustion of Engine Relevant Fuels with Emphasis on Soot Precursors. *Combustion and Flame* **2009**, *156* (3), 588–607. https://doi.org/10.1016/j.combustflame.2008.12.007.

34. Laidler, K. J. *Chemical Kinetics*; Pearson, (, 5Th Impression: New Delhi, 1987; pp. 276–346.

ACADEMIC VITA

Ethan Rys www.linkedin.com/in/ethan-rys-che

Process Engineer | Chemical Engineer

EDUCATION & PROFESSIONAL DEVELOPMENT

Bachelor of Science in Chemical Engineering | Pennsylvania State University – Schreyer Honors College

- **Expected Graduation:** 05/2022
- ***Extra-Curriculars****: AIChE, Atlas THON, Schreyer Success Mentor, Club Golf, Amateur Boxing Coach*
- ***Awards****: Earned Schreyer Honors College Scholarship and placed in the Top 20% of 2018 National MathWorks Modeling Challenges.*
- ***Thesis:*** *Efficient Utilization of Stranded Methane Resources – (estimated completion 04/22)*

PROFESSIONAL EXPERIENCE

LionTutors | PRIVATE AND CLASSROOM TUTOR – CHEMISTRY CLASSWORK 09/2019 to Present

- Tutor an average of 2-3 students each week by creating innovative and engaging lesson plans and activities based on differentiated learning needs.
- Tutoring formats include both one-on-one sessions as well as larger group reviews of 10-15 students.

INTERNSHIPS

Pennsylvania State University | COMPUTATIONAL CATALYSIS – UNDERGRADUATE RESEARCH STUDENT 01/2021 to Present

- *Research Director*: Dr. Alexopoulos and Dr. Janik
- Investigate and draw actionable hypotheses and conclusions to maximize the chemical conversion of methane and biogas while achieving the most desirable ratio of selectivity for value-added products.
- Model and implement the addition of heterogenous single-atom catalysts to provide shorter reaction pathway for carbon coupling in biogas. Models are based on density-functional theory (DFT) calculations performed through UNIX.
- Utilized Chemkin Pro software to model equilibria and plug-flow reactor (PFR) simulations for optimal reaction conditions by manipulating system variables such as temperature profiles, reactor size, and residence time.

Wabtec | PROCESS ENGINEER – WASTEWATER TREATMENT INTERN 05/2021 to 07/2021

- Employed data-drive insights to develop process model in Microsoft Excel for oil sensor analytics and ensure engine reliability.
- Served as the primary assistant to the Senior Facility Manager (SFM), fulfilling day-to-day operations such as directing waste hauling and safe chemical/maintenance procedures while the SFM was on medical leave.
- Conceived and implemented chemical safety protocols to address chemical handling accidents prior to facility arrival.
- Improved cross-functional collaboration by liaising with multiple departments including engineering, quality control, material sourcing, and Environmental Health & Safety (EHS) to expand teamwork and communication initiatives.

GE Transportation – A Wabtec Company | PROCESS ENGINEER – WASTEWATER TREATMENT INTERN 05/2019 to 08/2019

- Assessed and reviewed procedures of wastewater treatment facilities to identify process gaps related to flock buildups, pH control, equipment maintenance, and chemical storage.
- Performed water sampling analysis of wastewater system to confirm economic viability of current chemicals and dosages.
- Interfaced with technicians and system operators to improve understanding of process dynamics and system maintenance.